



UNIVERSITY OF LEEDS

This is a repository copy of *Cotton nonwovens with unidirectional water-transport properties produced by atmospheric plasma deposition*.

White Rose Research Online URL for this paper:

<https://eprints.whiterose.ac.uk/171882/>

Version: Accepted Version

---

**Article:**

Pu, Y, Yang, J, Russell, SJ [orcid.org/0000-0003-0339-9611](https://orcid.org/0000-0003-0339-9611) et al. (1 more author) (2021) Cotton nonwovens with unidirectional water-transport properties produced by atmospheric plasma deposition. *Cellulose*, 28 (7). pp. 4427-4438. ISSN 0969-0239

<https://doi.org/10.1007/s10570-021-03794-x>

---

© The Author(s), under exclusive licence to Springer Nature B.V. part of Springer Nature 2021. This is an author produced version of a paper published in *Cellulose*. Uploaded in accordance with the publisher's self-archiving policy.

**Reuse**

Items deposited in White Rose Research Online are protected by copyright, with all rights reserved unless indicated otherwise. They may be downloaded and/or printed for private study, or other acts as permitted by national copyright laws. The publisher or other rights holders may allow further reproduction and re-use of the full text version. This is indicated by the licence information on the White Rose Research Online record for the item.

**Takedown**

If you consider content in White Rose Research Online to be in breach of UK law, please notify us by emailing [eprints@whiterose.ac.uk](mailto:eprints@whiterose.ac.uk) including the URL of the record and the reason for the withdrawal request.



[eprints@whiterose.ac.uk](mailto:eprints@whiterose.ac.uk)  
<https://eprints.whiterose.ac.uk/>

1 **Cotton Nonwovens with Unidirectional Water-**  
2 **Transport Properties Produced by**  
3 **Atmospheric Plasma Deposition**

4 Yi Pu<sup>1</sup>, Jing Yang<sup>1</sup>, Stephen J. Russell<sup>2</sup>, Xin Ning<sup>1\*</sup>

5 <sup>1</sup> *Shandong Center for Engineered Nonwovens, College of Textiles & Clothing, Qingdao University,*  
6 *Qingdao 266071, Shandong, P. R. China.*

7 <sup>2</sup> *School of Design, University of Leeds, Leeds, UK*

8 \*Corresponding Author: xning@qdu.edu.cn

9 **Abstract**

10 Cotton based nonwovens with unidirectional water-transport through the thickness of the fabric were  
11 prepared using atmospheric plasma technology. In controlling the plasma deposition parameters, a  
12 thin layer of polymerized Hexamethyldisiloxane was locally deposited onto a cotton nonwoven  
13 fabric, so that only the treated surface was hydrophobic, while the untreated surface remained  
14 hydrophilic. The water contact angle, surface morphology and chemical composition of the fabric  
15 surfaces were characterized, and the unidirectional water-transport performance, vapor transmission  
16 rate, thermal stability and durability of the treated nonwovens were tested. It was found that a super-  
17 hydrophobic surface could be durably achieved on one side of the fabric while maintaining a  
18 completely wettable surface on the other. The resulting asymmetric wettability enables the  
19 nonwovens to exhibit unidirectional water liquid-transport, without negatively affecting vapor  
20 transmission and air permeability. Such differential moisture management properties in sustainable  
21 cotton nonwovens are highly desirable for applications in hygiene, infection control and medical  
22 device applications.

23

24 **Keywords**

25 *Nonwoven fabric, plasma treatment, amphoteric, unidirectional water-transport.*

26

## 27 Introduction

28 Directional transport of liquids, whether relating to the management of bodily  
29 fluids in fabrics, transportation across biological membranes or nutrient transport  
30 in plants, is highly desirable in both nature and engineering applications (Zhao et  
31 al. 2017). Mechanical or capillary pressure and chemical potential are key driving  
32 forces governing the directional transmission phenomena of liquids, while fluid  
33 surface tension and wetting behaviour are also important factors. Amphoteric  
34 fabrics, also referred to as Janus materials, are those with the ability to direct the  
35 transport of liquid in one direction through differential surface functionalities.  
36 Asymmetric wetting properties include, for example, hydrophobic-hydrophilic,  
37 lipophilic-oleophobic, and amphoteric behaviour (Gore and Kandasubramanian  
38 2018). Such materials in the form of membranes have been described by Zhou and  
39 Guo (2019) (Zhou and Guo 2019), and herein, we refer to amphoteric and Janus  
40 materials interchangeably.

41 A difference in the surface energies between the two sides (or regions) of the  
42 same fabric or membrane results in asymmetric wettability, and also affects the  
43 inherent driving forces responsible for unidirectional water-transport (Yang et al.  
44 2018a). Generally speaking, Janus membranes can be divided into three categories:  
45 polymeric Janus membranes, polymeric-inorganic Janus membranes and inorganic  
46 Janus membranes (Zhou and Guo 2019). Textiles are valuable substrates for many  
47 Janus membranes because of their porous structure (Zhao et al. 2017). Such fibrous  
48 Janus membranes can be prepared as double-layer composite structures (Yang et al.  
49 2017), for example using layer-by-layer electrospinning (Gore and  
50 Kandasubramanian 2018; Wang et al. 2018; Wu et al. 2012), or through single-  
51 sided modification (Yang et al. 2018a) using a surface treatment (Yang et al. 2019b).  
52 Owing to their unidirectional water-transport functionality, Janus fabrics have been  
53 widely applied in fields such as oil-water separation (Gore and Kandasubramanian  
54 2018; Yue et al. 2018), fog collection (Ren et al. 2017), membrane distillation  
55 (Huang et al. 2017; Yang et al. 2017; Zhu et al. 2018) and blood plasma separation  
56 (Zhang et al. 2017) among others. In a fascinating new research paper, a “skin-like”  
57 fabric was demonstrated through controlled gradient wettability. The selectively  
58 treated hydrophilic channels amongst a hydrophobic substrate functioned like sweat  
59 glands in the human skin that repelled bulk liquid while allowing moisture  
60 transmission (Lao et al. 2020).

61 Although various strategies have been developed to modify the surface of  
62 membranes, the practical implementation of asymmetric modification of fabrics  
63 remains challenging. Wet chemistry easily penetrates through the thickness of many  
64 fabrics due to capillary effects, resulting in simultaneous chemical modification of  
65 both sides of the substrate. At least two methods can be implemented to address this:  
66 (a) introducing an extra interface on the surface of the fabric to separate the

67 modified layer from the unmodified layer and (b) applying a reaction gradient along  
68 the fabric uniformly (Yang et al. 2018a). However, a simpler approach is needed  
69 that allows for cost-effective localised treatment of fabric surfaces.

70 Atmospheric plasma treatment has attracted considerable attention due to its  
71 ease of use at ambient conditions. Modification of fabric surfaces is possible  
72 without changing the internal composition of the fibre. Highly reactive particles  
73 that participate in the plasma reaction, such as ions, free radicals, electrons and so  
74 on (Davis et al. 2011; Yang et al. 2018a), can physically or chemically react with  
75 the substrate without causing damage to the bulk of the material (Dowling et al.  
76 2011). The application of atmospheric pressure plasma jet processes also makes it  
77 possible to treat fabrics continuously (Li et al. 2017). Previously, researchers have  
78 prepared Janus membranes using vacuum plasma treatment (Airoudj et al. 2016;  
79 Teare et al. 2002; Yan et al. 2017), but continuous and large-scale production has  
80 not yet been achieved. In previous research, the continuous production of  
81 superhydrophobic cotton fabrics using HMDSO monomer by plasma treatment was  
82 demonstrated (Yang et al. 2019a; Yang et al. 2018b).

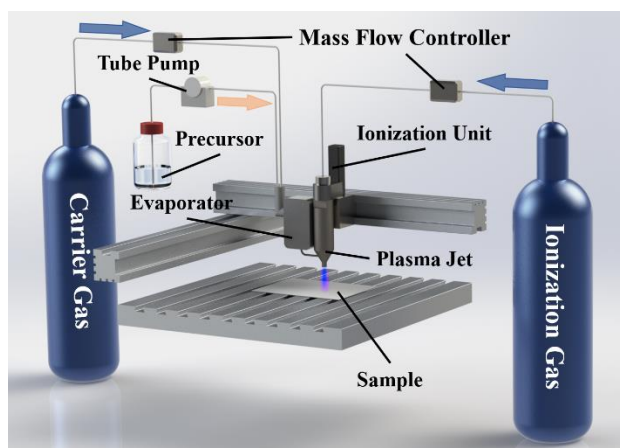
83 Herein, further research is reported exploring the preparation and behaviour of  
84 cotton nonwoven fabrics with amphoteric function, prepared by atmospheric  
85 pressure plasma treatment. By adjusting plasma jet treatment parameters,  
86 polymerized HMDSO was deposited on one side of the fabric, such that a  
87 continuous process compatible with industrial scale-up could be envisaged. The  
88 water contact angle, fibre surface morphology, and chemical composition of the two  
89 sides of the amphoteric fabric was analysed, and the directional water-transport  
90 behaviour, as well as vapor permeability, were characterized. To enable a fuller  
91 assessment of the utility of the resulting amphoteric effects, the thermal stability  
92 and durability of the treatments were also examined.

## 93 **Experimental**

### 94 **2.1. Materials**

95 Hexamethyldisiloxane (HMDSO,  $\geq 99.0\%$ , density=0.764 g/ml, boiling  
96 point=101 °C) was purchased from Shanghai Aladdin Chemical Co., Ltd, China.  
97 Cotton spunlaced nonwovens (80 g/m<sup>2</sup>, thickness=1 mm, density=80 kg/m<sup>3</sup>) were  
98 supplied by CHTC Jiahua Nonwoven Co., Ltd, China. The cotton fibres were first  
99 bleached before the hydroentanglement process, so the final fabrics were free from  
100 any sizing agent on the surfaces.

101 **2.2. Preparation of the Amphoteric Cotton Nonwovens**



102

103 **Fig. 1** Schematic Diagram of the Atmospheric Pressure Plasma System Operating with Computer-  
104 Controlled Motion and Velocity of the Plasma Jet

105

106

107

108

109

110

111

112

113

114

115

116

117

118

119

120

121

122

123

124

125

126

127

128

129

130

131

Amphoteric cotton nonwoven samples were prepared in a single step using an Atmospheric Pressure Plasma System (Model AS400 + PFW10, Plasma Treat GmbH, Steinhagen, Germany). The monomer (HMDSO) liquid was introduced into the afterglow region of the plasma by the carrier gas (Argon) after being heated to boiling point. HMDSO was polymerized by the energy provided by the plasma, and then deposited on to the surface of the nonwoven. By controlling the plasma process, the treated surface (TS) could be rendered hydrophobic while the untreated surface (UTS) remained hydrophilic. A schematic diagram of the Atmospheric Pressure Plasma System is shown in **Figure 1**, the gas was piped into the ionization unit, powered by an RF (21 kHz) power supply, to form the plasma. At the same time, the HMDSO precursor was piped into the evaporator via a tube pump. The temperature in the evaporator was slightly higher than the boiling temperature of the precursor. The carrier gas was directed to the evaporator and mixed with the vaporized precursor. The mixture was introduced into the afterglow region of the plasma and deposited on the surface of the nonwoven samples via the plasma jet after polymerization. The plasma jet was computer-controlled and traveled across the surface in an “S” shape. The plasma treatment is carried out under atmospheric pressure, and the movement of the plasma jet could be controlled. The precursor is directly introduced to the plasma jet for polymerization, so the sample can be prepared in one step. Industrialized large-scale production can be realized since the plasma jet is able to run continuously.

Compressed air was used as ionization gas; the voltage of the power supply was 300 V; the plasma cycle time (PCT), which influences the energy of the plasma was 60 %. Argon (Ar, 99.7%) was used as the carrier gas, and the flowrate was 300 L/h. In addition, the plasma jet scanning step distance was 2 mm and the distance between the nonwoven sample and jet nozzle was 40 mm.

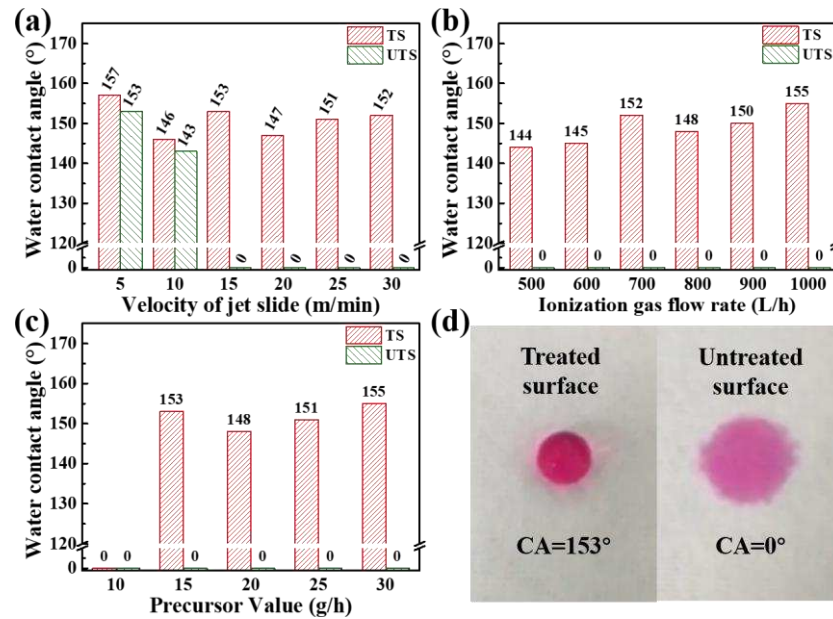
### 132 **2.3. Characterization**

133 Water contact angle was measured by a contact angle goniometer (JY-PHb,  
134 Hebei, China). Scanning Electron Microscopy (SEM, Phenom Pro, Phenom-World  
135 B.V., Netherlands) was employed to characterize the surface morphology of fibres  
136 in the resulting amphoteric cotton nonwoven fabrics. The chemical structure of the  
137 fabrics was characterized by Fourier Transform Infrared Spectroscopy (FTIR  
138 Spectrometer, Nicolet iS5, Thermo Company, USA). The repeated liquid strike-  
139 through time of the fabric was tested by a LISTER AC Liquid Strike Through Time  
140 Tester (Lenzing Instruments GmbH & Co. KG, Austria) according to the ERT  
141 153.0-02 standard. The wetback after a repeated strike-through time of the fabrics  
142 was tested by a WETBACK Nonwovens Wetback Tester (Lenzing Instruments  
143 GmbH & Co. KG, Austria) according to the ERT 154.0-02 standard. The water-  
144 vapor transmission rate was measured by a fabric moisture analyzer (YG601H-II,  
145 Zhejiang, China) according to GB/T 12704.2-2009. Air permeability was measured  
146 (Textest FX 3300-IV, Schwerzenbach, Switzerland) at a pressure of 200 Pa over an  
147 area of 20 cm<sup>2</sup>. The pore size distribution was characterized by a pore size meter  
148 (Topas PSM 165, Dresden, Germany). Topor (perfluoro compound, Topas specific  
149 testing fluid, surface tension 16 mN·m<sup>-1</sup>) was used as the wetting fluid, and the  
150 cross-sectional area of measurement was 0.95 cm<sup>2</sup>. Furthermore, fabric samples  
151 were stored at 90 °C and at -18 °C for one hour to determine the stability of the  
152 plasma treatment, and then for 2 months to assess the long-term durability.

## 153 **Results and Discussion**

### 154 **Effect of Plasma Treatment Parameters on the Amphoteric Properties**

155 Plasma treatment parameters are a major contributing factor to the modulation  
156 of amphoteric behaviour in fabrics. The face side of the cotton nonwoven fabric  
157 (treated surface, TS) was intended to be evenly coated by the treatment with  
158 HMDSO, whereas the reverse side (untreated surface, UTS) was expected to have  
159 remained untreated. The factors affecting the processing and penetrating  
160 performance of the plasma include the velocity of jet slide, the ionization gas flow  
161 rate and the precursor flow rate (Ekezie et al. 2019; Yang et al. 2018b). Therefore,  
162 the effect of these three parameters on the resulting amphoteric properties of the  
163 plasma treated cotton nonwovens was explored systematically, and the water  
164 contact angle was used to indicate a transformation to hydrophobic behaviour.



165

166 **Fig. 2** Water contact angle of the treated surface (TS) and untreated surface (UTS) of the cotton  
 167 nonwoven fabrics treated using different plasma parameters: (a) velocity of the jet slide; (b)  
 168 ionization gas flow rate; (c) precursor value (flow rate). The droplet wetting characteristics of the  
 169 TS and UTS, where CA = contact angle (d)

170

171 **Figure 2** reports the water contact angle of the TS and the UTS of the cotton  
 172 nonwoven fabrics, following modulation of three different plasma process  
 173 parameters. Firstly, the ionization gas flow rate and the precursor value were set to  
 174 700 L/h and 30 g/h, respectively, and the velocity of the jet slide was gradually  
 175 adjusted from 5 m/min to 30 m/min at an interval of 5 m/min. **Figure 2a** indicates  
 176 that both sides of the treated fabric are hydrophobic when the jet slide ran at a low  
 177 velocity, i.e., < 10 m/min, producing water contact angles of ~140-150°. As the jet  
 178 velocity increased to higher than 15 m/min, while the jet facing side (TS) continued  
 179 to exhibit high contact angles of around 150°, the contact of the reverse side (UTS)  
 180 of the nonwoven retained its original wettability (contact angle of 0°). The lack of  
 181 amphoteric effect at low jet slide velocity is the result of the polymerized HDMSO  
 182 being able to penetrate the porous structure of the cotton nonwoven due to the  
 183 longer jet dwell time. By increasing the jet slide velocity, the penetration of  
 184 polymerized HDMSO to the reverse side of the fabric was inhibited.

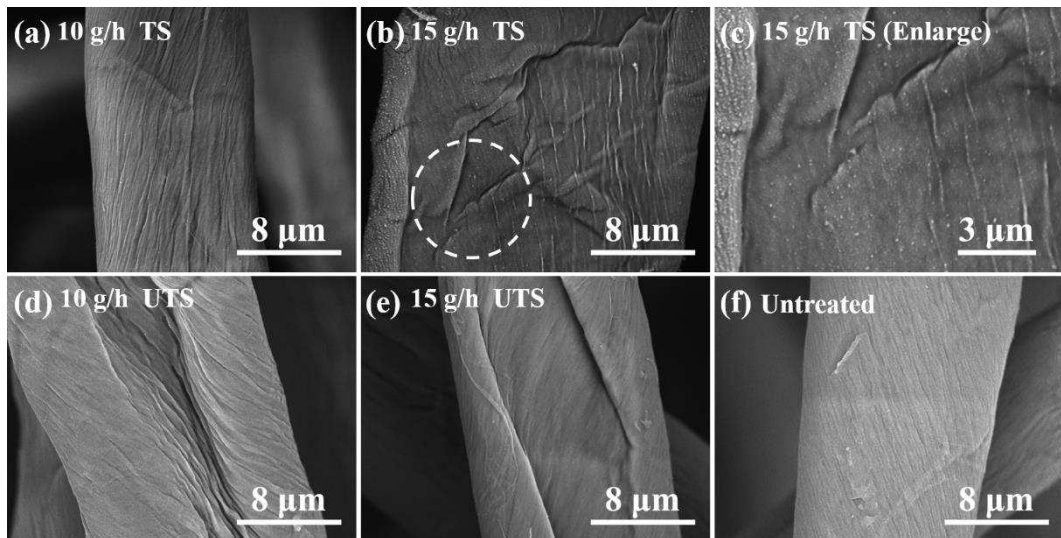
185

186 Then, the velocity of the jet slide was fixed at 30 m/min and the precursor  
 187 value was set to 30 g/h. As the ionization gas flow rate increased from 500 L/h to  
 188 1000 L/h, it was found that the treated cotton nonwovens were all amphoteric  
 189 (**Figure 2b**). However, the plasma glow was unstable when the ionization gas flow  
 190 rate was low, which may have an adverse impact on the uniformity of the  
 191 hydrophobic coating. Finally, the effect of the precursor value on the amphoteric  
 192 property was explored, wherein the velocity of the jet slide and the ionization gas  
 193 flow rate were fixed at 30 g/h and 1000 L/h, respectively. As is evident in **Figure**  
 194 **2c**, while the precursor value was at 10 g/h, the hydrophobic modification of the TS  
 was insufficient due to the small amount of precursor, leading to the hydrophilicity

195 remaining on both sides of the fabric. However, amphoteric behaviour was obtained  
196 at a higher precursor value ( $\geq 15$  g/h),

197 Based on these observations, to produce amphoteric cotton nonwoven fabrics,  
198 preferred values for the velocity of the jet slide, the ionization gas flow rate and the  
199 precursor were selected as 30 m/min, 1000 L/h and 15 g/h respectively. The water  
200 infiltration of the TS and UTS of the treated cotton nonwovens is shown in **Figure**  
201 **2d** and clearly highlights differences in the wetting and rate of lateral spreading of  
202 the liquid droplets in the fabric, consistent with amphoteric behaviour.

### 203 3.2 Surface Morphology



204  
205 **Fig. 3** SEM images of treated (TS) samples using different precursor values compared to the  
206 untreated cotton nonwoven fabric: 10 g/h TS (a); 15 g/h TS (b); 15 g/h enlarged TS (c); 10 g/h UTS  
207 (d); 15 g/h UTS (e); untreated control (f)  
208

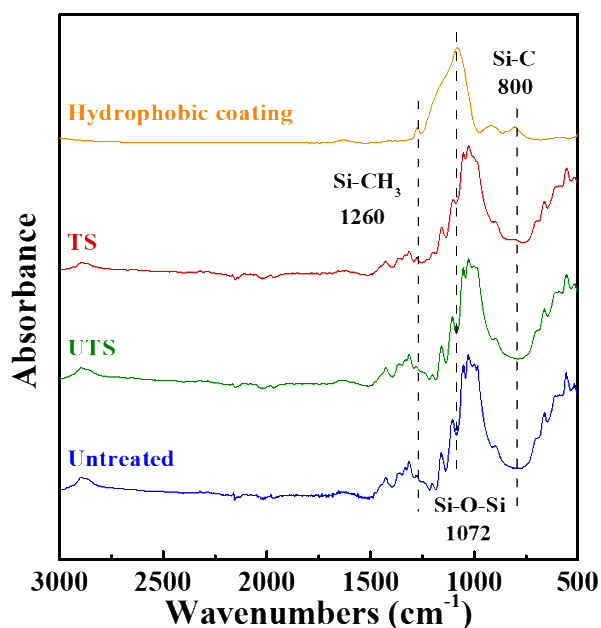
209 Plasma treatment applied to the surface of cotton nonwovens, may be expected  
210 to produce changes in fibre surface morphology, which could affect physical  
211 properties (Lee et al. 2000). **Figure 3** illustrates the resulting surface morphology  
212 of cotton fibres in each of the treated nonwoven fabrics, subjected to different  
213 precursor values (TS and UTS), together with the untreated cotton nonwoven  
214 control sample. It was found that for the treated fabric produced with a precursor  
215 value of 15 g/h, the fibres on the TS were evenly coated by the polymerized  
216 HMDSO. At higher magnification in the same sample (**Figure 3c**), uniform nano-  
217 protrusions on the fibre surfaces were observed. The formation of nano-protrusions  
218 is mainly due to the rapid replenishment of precursor in the plasma environment  
219 (Lazauskas et al. 2014). This coating was carefully scraped off the fibre surface and  
220 was found to be a white waxy coating. This polymer film is primarily responsible  
221 for the hydrophobic properties observed in the cotton nonwoven fabrics post plasma  
222 treatment, and the uniform nano-protrusions may also be expected to enhance  
223 hydrophobic properties (Kim and Lee 2019). The surface morphology of untreated  
224 fibres were very similar to that of TS fibre at a precursor value of 10 g/h, and



225 features such as nano-protrusions were generally absent. According to Palaskar  
226 (2011) (Palaskar et al. 2011), the surface coverage of the TS mainly depends on the  
227 value of the precursor. A small amount of precursor brings about a thin hydrophobic  
228 coating on the treated surface, which may be insufficient to yield a significant  
229 change in hydrophobicity. The surface morphology of fibres in the UTS of fabric  
230 samples that exhibited amphoteric behaviour were the same as those in the  
231 untreated sample. This confirms that the plasma did not penetrate the fabric  
232 structure, and therefore no hydrophobic coating was deposited on the UTS.

### 233 3.3 Chemical Components

234



235

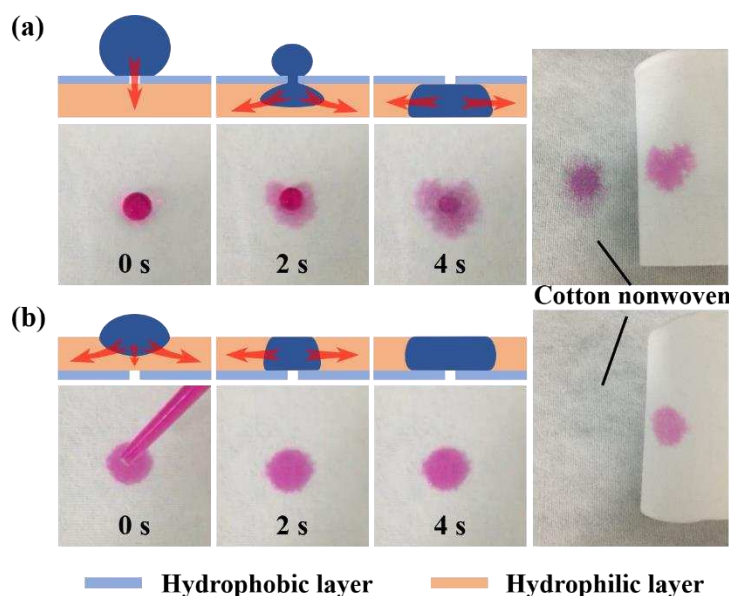
236 **Fig. 4** FTIR Spectra of the HMDSO coating material, coated amphoteric cotton nonwoven fabric  
237 (TS and UTS) and the untreated control fabric

238

239 The hydrophobic behaviour of plasma treated cotton nonwovens is largely  
240 related to their surface chemical composition. The FTIR spectra of the hydrophobic  
241 coating, amphoteric cotton nonwoven (both sides) and untreated cotton nonwoven  
242 are shown in **Figure 4**. The peak at 1072 cm<sup>-1</sup> is attributable to the stretching  
243 vibration of the Si-O-Si bond (Wallimann et al. 2018), present in the hydrophobic  
244 coating. It can also be observed that the infrared absorbance at this position in the  
245 TS of the amphoteric fabric is slightly higher than that in the UTS as well as in the  
246 untreated cotton nonwovens. Additionally, the peaks at 1260 cm<sup>-1</sup> and 800 cm<sup>-1</sup> are  
247 due to the bending vibration of the CH<sub>3</sub> and the Si-C rocking vibrations in Si-CH<sub>3</sub>,  
248 respectively (Bashir and Bashir 2015; Raynaud et al. 2005). These two peaks appear  
249 in the spectra of both the hydrophobic coating and the TS of the amphoteric  
250 nonwoven sample. Si-CH<sub>3</sub> groups in the plasma polymerization are low surface  
251 energy groups, that can be expected to impart hydrophobic properties (Kale and  
252 Palaskar 2011). It is also evident in **Figure 4** that these characteristic peaks are not

253 present in the spectra of the UTS of the amphoteric nonwovens, which is  
254 comparable to that of untreated cotton. Therefore, almost no polymerized HMDSO  
255 was found to be present on the UTS, enabling it to remain hydrophilic due to its  
256 cellulosic composition.

### 257 3.4 Unidirectional Water-Transport Behaviour



258

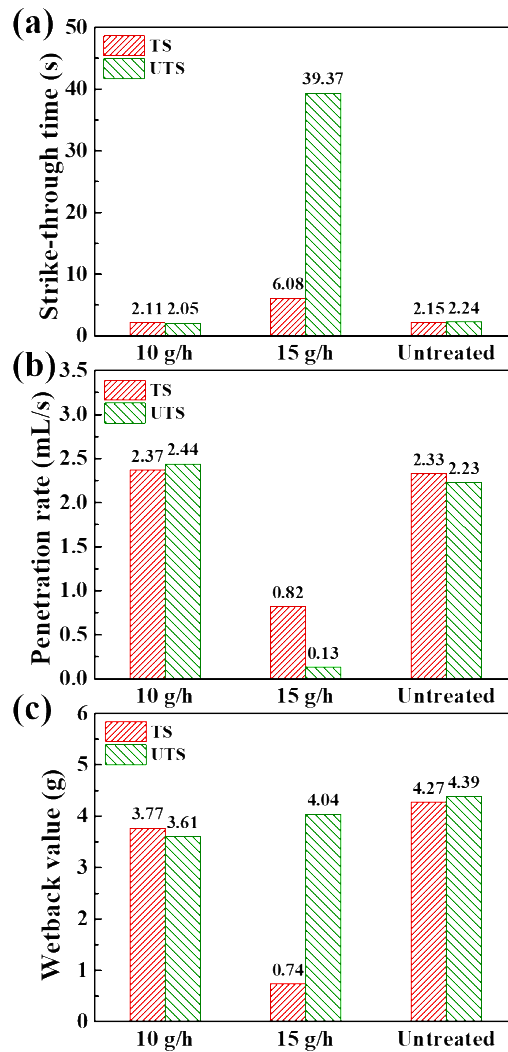
259 **Fig. 5** Unidirectional through thickness water-transport behaviour of amphoteric cotton nonwoven  
260 fabrics  
261

262 Janus fabrics have unidirectional water-transport functionality owing to their  
263 amphoteric properties (Wang et al. 2010). In other words, water can be transported  
264 from the hydrophobic surface to the hydrophilic surface but cannot be transported  
265 in reverse. Published literature has pointed out that the thickness of the hydrophobic  
266 coating has an influence on the performance of unidirectional water-transport in  
267 amphoteric fabrics. When the hydrophobic coating is too thin, the fabric has  
268 bidirectional transport behaviour, but when the hydrophobic coating is too thick,  
269 liquid transport can be impeded on both sides (Wang et al. 2019). Herein, treated  
270 cotton nonwoven fabrics produced using a precursor value of 15 g/h were found to  
271 have a hydrophobic coating with a suitable thickness to exhibit unidirectional  
272 water-transport functionality. The infiltration and penetration of water droplets in  
273 the TS and the UTS of the amphoteric cotton nonwoven fabric is shown in **Figure**  
274 **5**. The water penetration is illustrated by placing an untreated cotton nonwoven  
275 fabric under the amphoteric cotton nonwoven fabric sample. When the water was  
276 placed on the hydrophobic layer (the TS), it penetrates the surface and transports to  
277 the reverse side, then laterally spreads on the UTS. (**Figure 5a**) In contrast, when  
278 water was placed onto the hydrophilic untreated surface (the UTS), the liquid just  
279 spreads laterally and does not transport through-thickness to the reverse side of the  
280 fabric. (**Figure 5b**) The unidirectional water-transport behaviour in amphoteric  
281 cotton nonwoven fabrics is linked to the asymmetric wettability. In the case where

282 the hydrophobic layer is facing upward, the water droplet exhibits a large contact  
283 angle. The highly curved air/water interface is associated with pressure, as is known  
284 from the Young-Laplace equation (Zhou et al. 2020):

$$\Delta p = \gamma \left( \frac{1}{R_1} + \frac{1}{R_2} \right) \quad (1)$$

285 In **equation (1)**,  $\Delta p$  denotes the pressure difference between the inside and outside  
286 of the liquid surface, it is influenced by the surface tension coefficient  $\gamma$  and the  
287 curvature radius of the liquid surface  $R_1$  and  $R_2$ . This pressure and the hydrostatic  
288 pressure due to the gravity of water is enough to overcome the hydrophobic force  
289 on the surface of the hydrophobic layer. Due to the porosity of the amphoteric cotton  
290 nonwoven and the open pore structure at the surface, the hydrophobic coating is not  
291 continuous, which allows the water to reach the underlying hydrophilic layer (Zhou  
292 and Guo 2019). Capillary forces in the hydrophilic layer assist with the transport of  
293 the liquid, as well as with lateral spreading, depending on the fibre orientation  
294 within this fabric layer (Mao and Russell 2003a; Mao and Russell 2003b). In  
295 contrast, when the hydrophilic layer is upward, water is dropped on the hydrophilic  
296 layer, and the contact angle is 0. The resulting balance of forces means rapid liquid  
297 inlet, and capillary forces can spread the water within the hydrophilic layer. The  
298 hydrophobic layer effectively prevents full-thickness penetration through the fabric,  
299 so water is not able to penetrate through the hydrophobic side. This phenomenon is  
300 also akin to a “liquid diode” (Tian et al. 2012) and it makes amphoteric nonwovens  
301 valuable in many double-phase processes.



303

304 **Fig. 6** Repeated liquid strike-through time (a), liquid penetration rate (b), and wetback (c) of the  
 305 amphoteric and untreated cotton nonwoven fabrics

306

307 To characterize the unidirectional water-transport characteristics of the  
 308 amphoteric cotton nonwoven fabrics quantitatively, the repeated liquid strike-  
 309 through times and the wetback after repeated strikethroughs were measured. The  
 310 mean strike-through times obtained are given in **Figure 6a**, based on a water  
 311 volume of 5 mL. It was observed that for amphoteric cotton nonwovens (15 g/h),  
 312 the mean strike-through time from the TS to the UTS was 6.08 s, which was much  
 313 less than for the UTS to the TS. Owing to the unidirectional water-transport  
 314 characteristics of the amphoteric cotton nonwoven fabric, water readily penetrated  
 315 from the hydrophobic to the hydrophilic side, but penetration in reverse was  
 316 markedly slower. The fabrics treated with a precursor value of 10 g/h, with a thin  
 317 hydrophobic layer did not exhibit this unidirectional water-transport behaviour  
 318 (Zhou and Guo 2019), so the strike-through time was almost the same as that of the  
 319 untreated cotton nonwoven fabric, whether from the TS to the UTS or from the UTS

320 to the TS. The strike-through time can be quantified as the water penetration rate  
321 (**Figure 6b**).

322 The wetback after repeated strike-through time is shown in **Figure 6c**, the mean  
323 wetback value on the TS of the amphoteric cotton nonwovens was 0.74 g, which is  
324 much smaller than that measured for the UTS, and untreated cotton nonwovens.  
325 With reference to the Washburn equation (Zhang and Luo 2020) in **equation (2)**:

$$h = \sqrt{\frac{cr\sigma \cdot \cos\theta \cdot t}{2\eta}} \quad (2)$$

326  $h$  denotes the wicking height of water,  $c$  is the capillary shape factor,  $r$  is the  
327 average capillary radius;  $cr$  is a fixed value referred to as the formal radius.  $\sigma$   
328 denotes the surface tension of the liquid,  $\theta$  denotes the contact angle and  $\eta$  is  
329 liquid viscosity. Thus, the wicking height is related to the contact angle and when  
330 the water reaches the hydrophobic layer of the TS, the wicking height and capillarity  
331 are reduced due to the large contact angle, which impedes wetback from the UTS  
332 to TS. As a result, little water remains on the TS after inlet, and the surface can  
333 remain dry. When this amphoteric cotton nonwoven fabric is used to make wearable  
334 hygiene products, for instance, diapers, the hydrophobic surface will be close to  
335 human skin, so that liquid could be quickly transported from the hydrophobic side  
336 to the hydrophilic side. The hydrophobic surface close to the skin will remain dry  
337 due to the low wetback characteristics of the hydrophobic side of this amphoteric  
338 cotton fabric. The low wet back is a valuable property in the top sheets of wearable  
339 hygiene products, as well as humidity-control clothing.

### 340 **3.6 Water-Vapor Transmission Rate and Air Permeability**

341

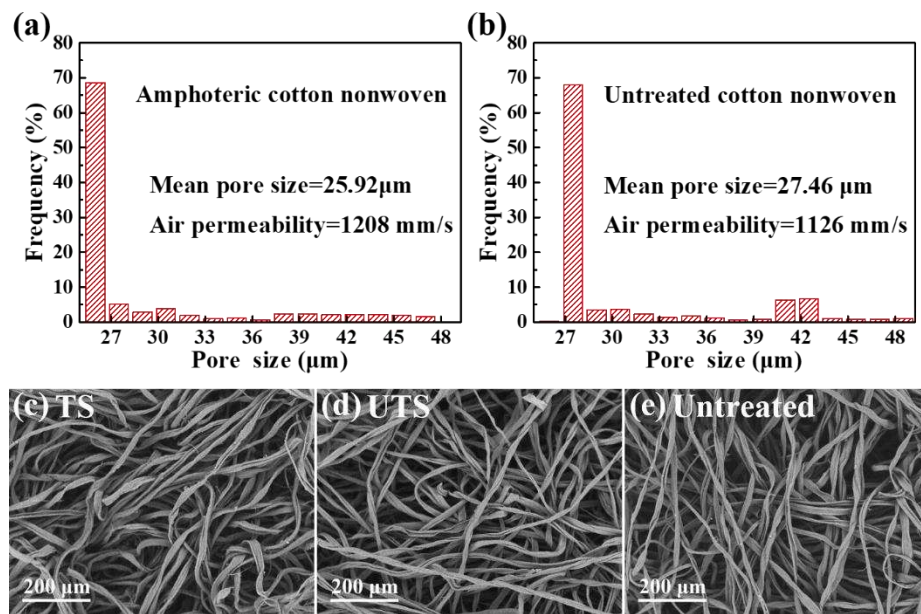
342 **Table 1.** Water-vapor transmission rate of amphoteric and untreated cotton nonwoven fabrics.  
343

Sample	Water-vapor transmission rate (WVT)
TS to UTS	191.007 g·(m <sup>2</sup> ·h) <sup>-1</sup>
UTS to TS	188.922 g·(m <sup>2</sup> ·h) <sup>-1</sup>
Untreated	185.371 g·(m <sup>2</sup> ·h) <sup>-1</sup>

344

345 The possible influence of the plasma treatment process on the water-vapor  
346 transmission rate and air permeability of the fabrics was also investigated. In Table  
347 1 it is evident that the water-vapor transmission rate in the amphoteric cotton  
348 nonwoven fabric was not significantly different from that of the untreated fabric at  
349 ~188 g·(m<sup>2</sup>·h)<sup>-1</sup>. We believe the differences might have been caused by sample  
350 handling during the treatment and characterization steps instead of real structural  
351 change to the porous fabric structures. Meantime, cotton fabrics could expand

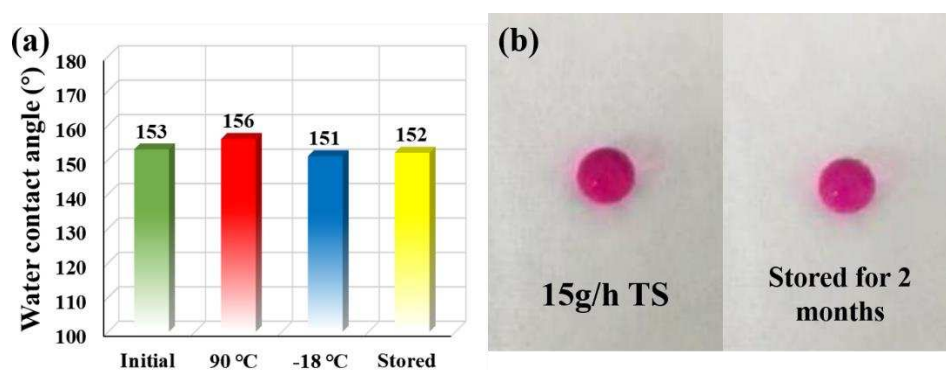
352 after absorbing moisture, which would have a certain impact on the water-vapor  
 353 transmission rate. However, this effect has an extremely limited influence on the  
 354 fabric and has almost no effect on the water-vapor transmission rate. The pore size  
 355 distributions and the Macro SEM image of the amphoteric cotton and the untreated  
 356 cotton nonwoven fabrics were also almost identical (**Figure 7**). It can be seen that  
 357 the fibrous assembling structure of the amphoteric cotton nonwoven and untreated  
 358 cotton nonwoven were not different, and both of the average pore sizes were about  
 359 26  $\mu\text{m}$ , confirming that plasma jet treatment resulted in no consolidation or  
 360 structural modification of the geometric structure of the fabric. Given that there was  
 361 no change in the fibrous structure, intrinsic permeability would not be expected to  
 362 be modified, and since water vapor molecules are much smaller than the pore size,  
 363 gas flow is highly unlikely to be affected by the hydrophobic layer and the change  
 364 in surface energy (Chemetov and Cipriano 2014). Similarly, no significant  
 365 difference in the air permeability between samples could be detected, with values  
 366 of 1208 mm/s and 1126 mm/s being obtained for the amphoteric cotton and  
 367 untreated cotton nonwoven fabrics respectively.



368  
 369  
 370  
 371  
 372

**Fig. 7** Pore size distribution and air permeability of amphoteric cotton nonwoven fabric (a) and untreated cotton nonwoven fabric (b); Macro morphology of the treated surface (c), untreated surface (d) and untreated cotton fabric (e).

### 373 3.7 Thermal Stability and Durability



374

375 **Fig. 8** Thermal stability and durability of the hydrophobic treatment in the amphoteric cotton  
376 nonwoven fabric (a). Photograph of water infiltration behaviour after 2 months storage  
377

378 Fugitive amphoteric behaviour, i.e., where the differential moisture handling  
379 characteristics are not durable, would limit industrial utility, so basic stability  
380 testing was performed in respect of thermal and temporal conditions (Lin et al.  
381 2019). The thermal stability and durability of the hydrophobic coating was  
382 characterized by measuring the water contact angle. As shown in **Figure 8**,  
383 following exposure to temperatures of 90 °C and -18 °C for one hour, and also  
384 storage in ambient conditions for two months, no marked differences were observed  
385 in the measured contact angles. Hydrophobicity remained quite consistent in the TS  
386 suggesting that cotton nonwoven fabrics treated in with HMDSO in the plasma jet  
387 process could be suitable for durable product applications in nonwovens where  
388 amphoteric behaviour is required.

### 389 Conclusion

390 Amphoteric cotton hydroentangled nonwoven fabrics with unidirectional  
391 water-transport functionality were successfully prepared by localised deposition of  
392 polymerized HMDSO through an optimised plasma jet process. Preferred treatment  
393 conditions were identified as 30 m/min, 1000 L/h and 15 g/h for the velocity of the  
394 jet slide, the ionization gas flow rate and the precursor rate, respectively. The treated  
395 side of the amphoteric cotton fabric was also characterised by the presence of nano-  
396 protrusions on the fibre surfaces. Asymmetric wetting and aqueous liquid transport  
397 were observed in amphoteric nonwoven fabric samples, and quantitatively  
398 characterized in repeated liquid strike-through and wetback studies. Liquid  
399 transport characteristics can be tuned by the modulation of plasma jet treatment  
400 process without affecting air permeability, vapor permeability or the pore size  
401 distribution of the nonwoven fabric. Furthermore, the polymerized HMDSO  
402 coating exhibited excellent thermostability and durability following storage, such  
403 that treated fabrics could be applied in a variety of industrial applications where  
404 moisture management is critical.

## 405 Authors' Contributions

406 **Yi Pu:** Initial conceptualization, Experiment, Data curation, Formal analysis, Methodology,  
407 Writing-Original draft, Writing-Review & editing; **Jing Yang:** Experiment, Writing-Review &  
408 editing; **Stephen Russell:** Formal analysis; Writing-Review & editing; **Xin Ning:** Initial  
409 conceptualization, Formal analysis, Funding acquisition, Methodology, Project administration,  
410 Resources, Writing-Review & editing.

## 411 Conflicts of Interest

412 All authors have given approval to the final version of the manuscript. The authors declare no  
413 conflicts of interest.

## 414 Funding

415 This research was supported by a start-up grant from the Qingdao University and by a grant on the  
416 establishment of the Shandong Center for Engineered Nonwovens (SCEN).

## 417 References

- 418 Airoudj A, Bally-Le Gall F, Roucoules V (2016) Textile with Durable Janus Wetting Properties  
419 Produced by Plasma Polymerization. *J Phys Chem C* 120:29162-29172.  
420 <https://doi.org/10.1021/acs.jpcc.6b09373>
- 421 Bashir M, Bashir S (2015) Hydrophobic-Hydrophilic Character of Hexamethyldisiloxane Films  
422 Polymerized by Atmospheric Pressure Plasma Jet. *Plasma Chem Plasma P* 35:739-755.  
423 <https://doi.org/10.1007/s11090-015-9623-z>
- 424 Chemetov NV, Cipriano F (2014) Inviscid limit for Navier-Stokes equations in domains with  
425 permeable boundaries. *Appl Math Lett* 33:6-11. <https://doi.org/10.1016/j.aml.2014.02.012>
- 426 Davis R, El-Shafei A, Hauser P (2011) Use of atmospheric pressure plasma to confer durable water-  
427 repellent functionality and antimicrobial functionality on cotton/polyester blend. *Surf Coat Tech*  
428 205:4791-4797. <https://doi.org/10.1016/j.surfcoat.2011.04.035>
- 429 Dowling DP, O'Neill FT, Langlais SJ, Law VJ (2011) Influence of dc Pulsed Atmospheric Pressure  
430 Plasma Jet Processing Conditions on Polymer Activation. *Plasma Process Polym.* 8:718-727.  
431 <https://doi.org/10.1002/ppap.201000145>
- 432 Ekezie FGC, Cheng JH, Sun DW (2019) Effects of atmospheric pressure plasma jet on the  
433 conformation and physicochemical properties of myofibrillar proteins from king prawn  
434 (*Litopenaeus vannamei*). *Food Chem* 276:147-156. <https://doi.org/10.1016/j.foodchem.2018.09.113>
- 435 Gore PM, Kandasubramanian B (2018) Heterogeneous wettable cotton based superhydrophobic  
436 Janus biofabric engineered with PLA/functionalized-organoclay microfibers for efficient oil-water  
437 separation. *J Mater Chem A* 6:7457-7479. <https://doi.org/10.1039/c7ta11260b>
- 438 Huang YX, Wang ZX, Jin J, Lin SH (2017) Novel Janus Membrane for Membrane Distillation with  
439 Simultaneous Fouling and Wetting Resistance. *Environ Sci Tech* 51:13304-13310.  
440 <https://doi.org/10.1021/acs.est.7b02848>
- 441 Kale KH, Palaskar S (2011) Atmospheric pressure plasma polymerization of hexamethyldisiloxane  
442 for imparting water repellency to cotton fabric. *Text Res J* 81:608-620.  
443 <https://doi.org/10.1177/0040517510385176>
- 444 Kim D-H, Lee D-H (2019) Effect of irradiation on the surface morphology of nanostructured  
445 superhydrophobic surfaces fabricated by ion beam irradiation. *Appl Surf Sci* 477:154-158
- 446 Lao L, Shou D, Wu YS, Fan JT (2020) "Skin-like" fabric for personal moisture management. *Sci*  
447 *Adv* 6:11. <https://doi.org/10.1126/sciadv.aaz0013>
- 448 Lazauskas A, Baltrusaitis J, Grigaliunas V, Jucius D, Guobiene A, Prosycevas I, Narmontas P (2014)  
449 Characterization of Plasma Polymerized Hexamethyldisiloxane Films Prepared by Arc Discharge.  
450 *Plasma Chem Plasma P* 34:271-285. <https://doi.org/10.1007/s11090-013-9516-y>
- 451 Lee HY, Park YH, Ko KH (2000) Correlation between surface morphology and  
452 hydrophilic/hydrophobic conversion of MOCVD-TiO<sub>2</sub> films. *Langmuir* 16:7289-7293.  
453 <https://doi.org/10.1021/la9915567>
- 454 Li J, Yuan Q, Chang X, Wang Y, Yin G, Dong C (2017) Deposition of organosilicone thin film from



455 hexamethyldisiloxane (HMDSO) with 50kHz/33MHz dual-frequency atmospheric pressure plasma  
456 jet. *Plasma Science & Technology* 19. <https://doi.org/10.1088/2058-6272/aa57e4>  
457 Lin X, Heo J, Choi M, Hong J (2019) Simply realizing durable dual Janus superwetable membranes  
458 integrating underwater low-oil-adhesive with super-water-repellent surfaces for controlled oil-water  
459 permeation. *J Membrane Sci* 580:248-255. <https://doi.org/10.1016/j.memsci.2019.03.038>  
460 Mao N, Russell SJ (2003a) Anisotropic liquid absorption in homogeneous two-dimensional  
461 nonwoven structures. *J Appl. Phys* 94:4135-4138. <https://doi.org/10.1063/1.1598627>  
462 Mao N, Russell SJ (2003b) Modeling permeability in homogeneous three-dimensional nonwoven  
463 fabrics. *Text Res J* 73:939-944. <https://doi.org/10.1177/004051750307301101>  
464 Palaskar S, Kale KH, Nadiger GS, Desai AN (2011) Dielectric Barrier Discharge Plasma Induced  
465 Surface Modification of Polyester/Cotton Blended Fabrics to Impart Water Repellency Using  
466 HMDSO. *J Appl. Polym. Sci* 122:1092-1100. <https://doi.org/10.1002/app.34237>  
467 Raynaud P, Despax B, Segui Y, Caquineau H (2005) FTIR plasma phase analysis of  
468 hexamethyldisiloxane discharge in microwave multipolar plasma at different electrical powers.  
469 *Plasma Processes Polym.* 2:45-52. <https://doi.org/10.1002/ppap.200400034>  
470 Ren FF et al. (2017) A single-layer Janus membrane with dual gradient conical micropore arrays for  
471 self-driving fog collection. *J Mater Chem A* 5:18403-18408. <https://doi.org/10.1039/c7ta04392a>  
472 Teare DOH et al. (2002) Pulsed plasma deposition of super-hydrophobic nanospheres. *Chem Mater*  
473 14:4566-4571. <https://doi.org/10.1021/cm011600f>  
474 Tian XL, Li J, Wang X (2012) Anisotropic liquid penetration arising from a cross-sectional  
475 wettability gradient. *Soft Matter* 8:2633-2637. <https://doi.org/10.1039/c2sm07111h>  
476 Wallimann R, Roth C, von Rohr PR (2018) Nanoparticle production from HMDSO in atmospheric  
477 pressure argon-oxygen plasma. *Plasma Processes Polym.* 15:8.  
478 <https://doi.org/10.1002/ppap.201700202>  
479 Wang H, Niu H, Zhou H, Wei X, Yang W, Lin T (2019) Multifunctional Directional Water Transport  
480 Fabrics with Moisture Sensing Capability. *ACS Appl. Mater Interfaces* 11:22878-22884.  
481 <https://doi.org/10.1021/acsami.9b06787>  
482 Wang HX, Ding J, Dai LM, Wang XG, Lin T (2010) Directional water-transfer through fabrics  
483 induced by asymmetric wettability. *J Mater Chem* 20:7938-7940.  
484 <https://doi.org/10.1039/c0jm02364g>  
485 Wang ZC, Li YG, Li SH, Guo J, Zhang SB (2018) Janus porous membrane with conical nanoneedle  
486 channel for rapid unidirectional water transport. *Chem Comm* 54:10954-10957.  
487 <https://doi.org/10.1039/c8cc05642k>  
488 Wu J, Wang N, Wang L, Dong H, Zhao Y, Jiang L (2012) Unidirectional water-penetration composite  
489 fibrous film via electrospinning. *Soft Matter* 8:5996-5999. <https://doi.org/10.1039/c2sm25514f>  
490 Yan XJ, Li JW, Yi LM (2017) Fabrication of pH-responsive hydrophilic/hydrophobic Janus cotton  
491 fabric via plasma-induced graft polymerization. *Mater Lett* 208:46-49.  
492 <https://doi.org/10.1016/j.matlet.2017.05.029>  
493 Yang HC, Xie YS, Hou JW, Cheetham AK, Chen V, Darling SB (2018a) Janus Membranes: Creating  
494 Asymmetry for Energy Efficiency. *Adv Mater* 30:11. <https://doi.org/10.1002/adma.201801495>  
495 Yang HC, Zhong WW, Hou JW, Chen V, Xu ZK (2017) Janus hollow fiber membrane with a mussel-  
496 inspired coating on the lumen surface for direct contact membrane distillation. *J Membrane Sci*  
497 523:1-7. <https://doi.org/10.1016/j.memsci.2016.09.044>  
498 Yang J, Pu Y, He HW, Cao RG, Miao DG, Ning X (2019a) Superhydrophobic cotton nonwoven  
499 fabrics through atmospheric plasma treatment for applications in self-cleaning and oil-water  
500 separation. *Cellulose* 26:7507-7522. <https://doi.org/10.1007/s10570-019-02590-y>  
501 Yang J, Pu Y, Miao DG, Ning X (2018b) Fabrication of Durably Superhydrophobic Cotton Fabrics  
502 by Atmospheric Pressure Plasma Treatment with a Siloxane Precursor. *Polymers* 10:13.  
503 <https://doi.org/10.3390/polym10040460>  
504 Yang XB, Yan LL, Ran FT, Pal A, Long J, Shao L (2019b) Interface-confined surface engineering  
505 constructing water-unidirectional Janus membrane. *J Membrane. Sci* 576:9-16.  
506 <https://doi.org/10.1016/j.memsci.2019.01.014>  
507 Yue XJ, Zhang T, Yang DY, Qiu FX, Li ZD (2018) Janus ZnO-cellulose/MnO<sub>2</sub> hybrid membranes  
508 with asymmetric wettability for highly efficient emulsion separations. *Cellulose* 25:5951-5965.  
509 <https://doi.org/10.1007/s10570-018-1996-8>  
510 Zhang DR, Luo R (2020) An alternative method to evaluate the surface free energy of mineral fillers  
511 based on the generalized Washburn equation. *Const. Build Mater* 231:8.  
512 <https://doi.org/10.1016/j.conbuildmat.2019.117164>  
513 Zhang WB, Hu L, Chen HM, Gao SJ, Zhang XC, Jin J (2017) Mineralized growth of Janus  
514 membrane with asymmetric wetting property for fast separation of a trace of blood. *J Mat Chem B*  
515 5:4876-4882. <https://doi.org/10.1039/c7tb00644f>  
516 Zhao Y, Wang HX, Zhou H, Lin T (2017) Directional Fluid Transport in Thin Porous Materials and

517 its Functional Applications. *Small* 13:22. <https://doi.org/10.1002/smll.201601070>  
518 Zhou H, Guo ZG (2019) Superwetting Janus membranes: focusing on unidirectional transport  
519 behaviours and multiple applications. *J Mater Chem A* 7:12921-12950.  
520 <https://doi.org/10.1039/c9ta02682g>  
521 Zhu R et al. (2020) Biomimetic Fabrication of Janus Fabric with Asymmetric Wettability for Water  
522 Purification and Hydrophobic/Hydrophilic Patterned Surfaces for Fog Harvesting. *ACS Applied*  
523 *Materials* 12:50113-50125. <https://doi.org/10.1021/acsami.0c12646>  
524 Zhou Y et al. (2020) Pressure difference-induced synthesis of P-doped carbon nano bowls for high-  
525 performance supercapacitors. *Chem Eng. J* 385:11. <https://doi.org/10.1016/j.cej.2019.123858>  
526 Zhu ZG, Liu ZQ, Zhong LL, Song CJ, Shi WX, Cui FY, Wang W (2018) Breathable and  
527 asymmetrically superwetable Janus membrane with robust oil-fouling resistance for durable  
528 membrane distillation. *J Membrane Sci* 563:602-609. <https://doi.org/10.1016/j.memsci.2018.06.028>